Numerical Simulation of the Nonequilibrium Diffuse Double Layer in Ion-Exchange Membranes

J. A. Manzanares,[+,§] W. D. Murphy,[†] S. Mafé,[+,§] and H. Reiss*[,†]

Department of Chemistry, University of California, Los Angeles, California 90024, and Rockwell International, Science Center Division, Thousand Oaks, California 91360

Received: March 30, 1993; In Final Form: May 12, 1993

We have analyzed theoretically the complex phenomena taking place when an electric current passes through the nonequilibrium diffuse double layer at the ion-exchange membrane/solution interface. Interesting results arise due to the nonlinear character of the system of equations consisting of the Nernst–Planck and Poisson equations, and the inhomogeneous nature of the membrane system (membrane plus bathing solutions). Some of these results confirm the conclusions concerning the space-charge distribution obtained previously by other authors using different methods. Others provide new physical insights into problems such as the question of the validity of the Donnan equilibrium relations at the membrane/solution interfaces, and the selectivity of ion-exchange membranes.

Introduction

Transport through ion-exchange membranes is of great scientific and technological importance. The full theory of this phenomenon presents some very difficult problems, so that even at this late date certain fundamental issues have not been satisfactorily resolved. The continuity equation governing the transport, involving a flux density prescribed by the well-known Nernst–Planck equation, is unfortunately nonlinear. Furthermore, the boundary conditions that must be included in the full description of the problem present their own set of difficulties and uncertainties. For the most part, the problems associated with the boundaries have been swept under the carpet and it has more often than not been assumed that instantaneous local equilibrium is established across an interface between the membrane and a bathing electrolyte solution. Whether this is always true, and if not, under what conditions does the assumption fail, have never been thoroughly examined, although various authors have made some attempts in this direction.[1] The question can only be studied by examining the structure of the interfacial zone, including that of the diffuse space charge layer in the bathing electrolyte.

The proper approach to this study involves more than the brute force numerical solution of the nonlinear initial and boundary value problem, including transport through the interfacial zone that emerges. In fact, it is necessary to introduce physically consistent boundary conditions, e.g., one must follow the evolution of boundary behavior through the transient period that precedes the establishment of steady-state transport. In this paper we examine these several questions and then introduce a numerical means for generating physically consistent solutions to the problem.

Although we are not here concerned with electrode behavior, techniques that we have used previously to solve the time evolution of a redox system[2] can be usefully applied to the membrane system. The main features of this method of numerical integration make it suitable for the study of any transport processes through spatial regions where large gradients in the physical variables (concentrations and electric potential) occur. In this sense, the present study is useful for demonstrating the applicability of the numerical procedure for a situation physically and mathematically different from that studied in ref 2. However, the chief focus of the present paper is not on numerical methods but rather on establishing a consistent physics of membrane transport at the same time that a very fundamental problem of membrane electrochemistry is studied. This problem involves the *structure of the electrical double layer (EDL) in the overlimiting current regime*, i.e., under extremely nonequilibrium conditions. Moreover, the complex phenomena associated with the passage of an electric current through the diffuse double layer are of considerable basic interest[1,3-6] and markedly influence the efficiency of membrane processes like electrodialysis.[7,8] Therefore, we endeavor to relate our results to previous ones in the field, while emphasizing those cases where new physical insights arise.

The steady-state nonequilibrium diffuse double layer at an electrode has been thoroughly studied (see ref 9 and, especially, ref 10 and references therein); however, such studies have not been performed for ion-exchange membranes.[1,3,5] Our analysis goes beyond these previous studies in the following ways: (i) the *whole* membrane system (membrane, electrical diffuse double layers, and diffusion boundary layers) is considered over a wide range of finite membrane thickness rather than only the polarized membrane/solution interface, (ii) our numerical procedure permits the imposition of conditions on the electric current and the electric potential, (iii) nonideal permselective membranes can be studied, and (iv) both steady-state and transient responses are dealt with. Our results reveal considerable influence of space charge on ion transport and some of our conclusions confirm the ideas previously advanced by Buck[10] for the case of electrodes, and Rubinstein[3] for the case of membranes, both of whom used different approaches. Others provide new physical insights into the behavior of the limiting current, into the applicability, during transport, of the equilibrium Donnan relationship to the membrane/solution interface, and into the permselectivity of the membrane.

From the point of view of the mathematical computations, we could consider both negatively and positively charged ion-exchange membranes. However, the transport mechanisms in the overlimiting current regime seem to depend very much on the particular charged groups considered.[3,4,8,11] In particular, water dissociation effects are more likely to occur in anion-exchange membranes than in cation-exchange membranes. We will consider here the changes in the structure of the electrical double layer at the membrane/solution interface as the mechanism responsible for the passage of overlimiting currents and, consequently, the study will be restricted to cation-exchange membranes.[3]

* To whom correspondence should be addressed.
+ University of California.
§ Permanent address: Department of Thermodynamics, University of Valencia, 46100 Burjasot, Spain.
† Rockwell International.

0022-3654/93/2097-8524$04.00/0

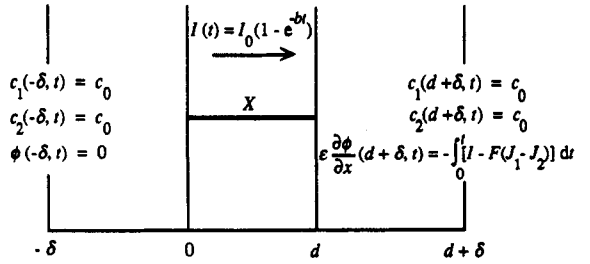

Figure 1. Schematic view of the whole membrane system (not to scale) and the boundary conditions imposed for the problem of the nonequilibrium EDL.

Formulation of the Problem

The membrane system under study is constituted by an ion-exchange membrane that extends from $x = 0$ to $x = d$ and two diffusion boundary layers (DBLs) that extend from $x = -\delta$ to $x = 0$ and from $x = d$ to $x = d + \delta$. The membrane is bathed by two bulk solutions with the same concentration c_0 of a 1:1 binary electrolyte. It will be assumed that the membrane contains fixed negatively charged groups at a uniform concentration X.

The principal equations involved in this time-dependent transport problem are the Nernst–Planck equations

$$J_i = -D\left[\frac{\partial c_i}{\partial x} + (-1)^{i+1} c_i \frac{F}{RT}\frac{\partial \phi}{\partial x}\right], \quad i = 1, 2 \tag{1}$$

the continuity equations

$$\frac{\partial J_i}{\partial x} = -\frac{\partial c_i}{\partial t}, \quad i = 1, 2 \tag{2}$$

the equation for the total electric current density including the displacement current[2,12]

$$I = F(J_1 - J_2) - \epsilon \frac{\partial^2 \phi}{\partial x\, \partial t} \tag{3}$$

and the Poisson equation

$$\frac{\partial^2 \phi}{\partial x^2} = -\frac{\rho}{\epsilon} = -\frac{F}{\epsilon}\begin{cases}(c_1 - c_2 - X), & 0 \le x \le d \\ (c_1 - c_2), & -\delta < x < 0 \text{ and } d < x < d + \delta\end{cases} \tag{4}$$

Here $J_i(x,t)$, D, and $c_i(x,t)$ denote the flux, diffusion coefficient, and local molar concentration of the ith species, respectively. (D is assumed to be the same for both ions because we are not interested in effects due to their different mobilities.) Subscript 1 refers to cations (counterions) and subscript 2 to anions (co-ions). The electric potential is represented by $\phi(x,t)$, the space-charge density by $\rho(x,t)$, the electric current density by $I(t)$, and the dielectric permittivity of the solution by ϵ. The symbols F, R, and T represent the Faraday constant, the gas constant, and the absolute temperature, respectively. Solvent flow and activity coefficients effects are neglected.

These transport equations are solved only in terms of the two ionic concentrations and the electric potential. Thus, the ion fluxes are eliminated from eqs 1 and 2, giving rise to eq 5 and

$$\frac{\partial c_i}{\partial t} = D\frac{\partial}{\partial x}\left[\frac{\partial c_i}{\partial x} + (-1)^{i+1} c_i \frac{F}{RT}\frac{\partial \phi}{\partial x}\right], \quad i = 1, 2 \tag{5}$$

these are solved together with eq 4. Figure 1 is a schematic view of the system and includes the boundary conditions imposed on eqs 4 and 5 at $x = -\delta$ and $x = d + \delta$. The system is considered to be electrically neutral at the outer boundaries of the DBLs, so that c_1 and c_2 have there the concentration c_0 of the bulk electrolyte solution. The condition $\phi(-\delta,t) = 0$ defines the reference level for the electric potential. The boundary condition for ϕ at $x = d + \delta$ merits a detailed explanation. First, note that Figure 1 also shows the electric current density that will be *imposed* through the membrane system, namely

$$I(t) = I_0(1 - e^{-bt}) \tag{6}$$

This current does not reach its steady value I_0 immediately, but after a characteristic time $t \approx 1/b$. This time dependence is thought to represent a good approximation to many experimental situations. Since I is not a function of x, it can be specified at any point in the system and, in particular, at the right boundary. Then, eq 3 establishes a boundary condition for the time evolution of $\partial\phi/\partial x$ at $x = d + \delta$. This boundary condition can be written as

$$\epsilon \frac{\partial^2 \phi}{\partial x\, \partial t}\bigg|_{(d+\delta,t)} = I(t) + FD\left[\left(\frac{\partial c_1}{\partial x} + c_1 \frac{F}{RT}\frac{\partial \phi}{\partial x}\right) - \left(\frac{\partial c_2}{\partial x} - c_2 \frac{F}{RT}\frac{\partial \phi}{\partial x}\right)\right]\bigg|_{(d+\delta,t)} \tag{7}$$

and plays a central role in the solution of the problem.

It is also necessary to specify the initial profiles of c_1, c_2, and ϕ. Since our main concern is the study of the EDL under nonequilibrium conditions, it seems appropriate to regard the system as being at equilibrium (zero ionic fluxes and current) at time $t = 0$. The description of this equilibrium state it is not straightforward when space-charge effects are retained, i.e., if we seek for an initial state incorporating the equilibrium EDLs at the two membrane/electrolyte interfaces.[13] There appear to be two possibilities. The first involves the inclusion and solution of the Poisson–Boltzmann equation.[14] However, this procedure involves either the use of an additional numerical method or, if an analytical approach is taken, the introduction of approximations (e.g., a perturbation approach that considers the electric potential as the sum of that at the center of the membrane and a term much smaller than unity). The second possibility is to generate the equilibrium state from eqs 4 and 5 and the appropriate boundary conditions (*not* those in Figure 1, which are specific for the study of the nonequilibrium EDL). We have followed the second alternative. This implies the solution of another transport problem prior to the one of interest. As already mentioned above, the transport equations are the same, but it is still necessary to specify the boundary conditions and initial state for this first problem. These are

$$\frac{\partial c_1}{\partial x}(-\delta,t) = \frac{\partial c_2}{\partial x}(-\delta,t) = 0, \quad \frac{\partial \phi}{\partial x}(-\delta,t) = 0, \quad \phi(-\delta,t) = 0$$

$$\frac{\partial c_1}{\partial x}(d+\delta,t) = \frac{\partial c_2}{\partial x}(d+\delta,t) = 0, \quad \frac{\partial \phi}{\partial x}(d+\delta,t) = 0 \tag{8}$$

and

$$c_1(x,0) = \begin{cases}X/2 + [(X/2)^2 + c_0^2]^{1/2}, & 0 \le x \le d \\ c_0, & -\delta \le x < 0 \text{ and } d < x \le d + \delta\end{cases}$$

$$c_2(x,0) = \begin{cases}-X/2 + [(X/2)^2 + c_0^2]^{1/2}, & 0 \le x \le d \\ c_0, & -\delta \le x < 0 \text{ and } d < x \le d + \delta\end{cases}$$

$$\phi(x,0) = \frac{RT}{F}\begin{cases}\ln\{-X/2c_0 + [(X/2c_0)^2 + 1]^{1/2}\}, & 0 \le x \le d \\ 0, & -\delta \le x < 0 \text{ and } d < x \le d + \delta\end{cases} \tag{9}$$

Equations 9 correspond to the well-known Donnan equilibrium relations, which assume that the ionic concentrations and the electric potential are uniform up to, but discontinuous at, the membrane/solution interfaces.

This first problem is solved out to very large times ($t \to \infty$) and the stationary profiles obtained are taken to be the initial profiles at $t = 0$ for the nonequilibrium, transport problem of interest (i.e., eqs 4 and 5 subject to the boundary conditions in Figure 1).

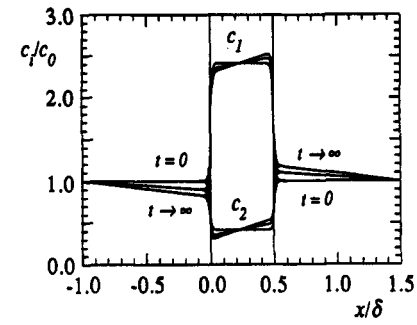

Figure 2. Concentration profiles corresponding to the passage of an electric current $I(t) = (1 - e^{-t/\tau_d})(2FDc_0/\delta)$ for times $t = 0, \tau_d$, and ∞. The values $\delta = 2d = 100\ \lambda$, and $c_0 = 0.5X$ have been used.

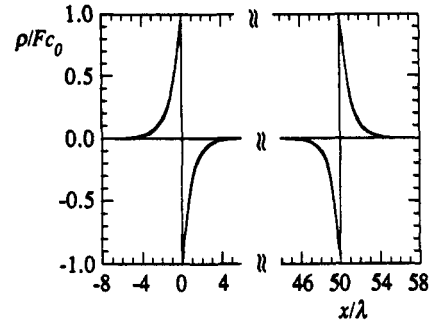

Figure 3. Detail of the space-charge concentration profiles at the two membrane/solution interfacial regions corresponding to the profiles in Figure 2. The space-charge concentration profile does not change appreciably with the passage of electric current.

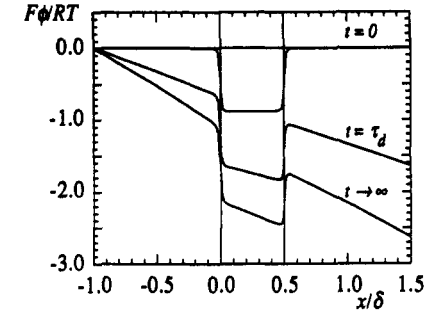

Figure 4. Electric potential profiles corresponding to the situation in Figure 2.

By proceeding in this way, the initial profiles for the second problem exhibit the expected space-charge effects at the membrane/solution interfaces, while the *total* charge stored in the membrane system is still zero.

Note that at $x = -\delta$, both the Dirichlet condition ($\phi(-\delta,t) = 0$) and a Neumann condition ($((\partial\phi/\partial x)(-\delta,t) = 0$) are prescribed when only one is necessary (see eqs 8). The Neumann condition alone sometimes leads to instabilities that do not occur when the Dirichlet condition is applied. We make use of both conditions by employing the Neumann condition in the discretization of eqs 5 and imposing the Dirichlet condition in the integration procedure. The integration procedure is described briefly in the Appendix.

Results

Before presenting the results, it is important to call attention to two details. First, the numerical method and the computer capability force the consideration of somewhat unrealistic systems (very thin membranes, but still much larger in thickness than the Debye length). However, the results can be considered as representative of the behavior of real synthetic membranes. Second, instead of specifying the values of all the membrane system parameters (ϵ, D, c_0, X, d, δ, etc.), we specify here only the values of dimensionless groups of parameters. Consistently, the results are presented in the form of dimensionless groups. For instance, the electric current density is given in units of (FDc_0/δ). This procedure gives results of greater generality and, at the same time, properly scales the numbers introduced in the computer code.

Figure 2 exhibits the concentration profiles in the system at $t = 0$, $t = 1/b = \tau_d$, and $t \to \infty$. Here $\tau_d \equiv \delta^2/D$ is the diffusional relaxation time. The polarization effects are apparent in the bulk of the DBLs. The electroneutral concentration profiles decrease linearly with position from $x = -\delta$ to $x \approx 4\lambda$ due to the positive applied electric current, where $\lambda \equiv [\epsilon RT/F^2X]^{1/2}$ is the Debye length in the membrane solution. At $x \approx 4\lambda$, EDL effects predominate and large deviations from local electroneutrality occur before the bulk of the membrane phase is reached, typically after several Debye lengths. Similar results are seen for the interface at $x = d$ with the only difference that the ion concentrations are higher at $x = d$ than at $x = d + \delta$. In fact, the use of the assumption of local electroneutrality in the bulk of the DBLs readily leads to the equations

$$c_1 = c_2 = c_0 - \frac{J_1 + J_2}{2D}(x + \delta), \quad -\delta \le x < 0$$

$$c_1 = c_2 = c_0 + \frac{J_1 + J_2}{2D}(d + \delta - x), \quad d < x \le d + \delta \qquad (10)$$

The charge density corresponding to the concentration profiles in Figure 2 is exhibited in Figure 3. The profiles for ρ in Figure 3 correspond to the times involved in Figure 2. Note that this figure reflects, in detail, the two EDLs at the membrane/solution interfaces. This charge density is typical for a negatively charged membrane and seems to be rather insensitive to an increase in the electric current. This is usually the case when the imposed electric current generates electric fields that are much smaller than those in the interfacial regions. However, the small changes of ρ with $I(t)$ in Figure 3 do result in *dramatic* changes in the electric potential, as is shown in Figure 4. Since we have assumed no difference in the ionic diffusion coefficients, Figure 4 shows the ohmic drops in the three bulk regions as well as the interface potentials. The potential varies almost linearly with position in these three bulk regions, as would be expected from the small relative changes in the ionic concentrations (see Figure 2). However, the behavior in the interfacial regions reveals a very important fact. If we extrapolate the two linear behaviors of the electric potential on each side of any interface, and compare the extrapolated potential difference, $F|\Delta\phi(t)|/RT$, with the equilibrium Donnan potential, $F|\Delta\phi_D|/RT = 0.88$, we notice that (i) it departs from the equilibrium value as the electric current increases, and (ii) it is higher than the equilibrium difference at the left and smaller at the right interface. In particular, the extrapolated potential difference takes the values $F\Delta\phi(0)/RT = -0.88$, $F\Delta\phi(\tau_d)/RT = -0.95$, and $F\delta\phi(\infty)/RT = -1.01$ at the left interface, and $F\Delta\phi(0)/RT = 0.88$, $F\Delta\phi(\tau_d)/RT = 0.81$, and $F\Delta\phi(\infty)/RT = 0.76$ at the right interface. These results can be rationalized easily. One would expect to have larger deviations from equilibrium at the left interface, because it is the polarization of this interface which leads to a limiting current. The differences quoted above are quite important since they provide a quantitative idea of the deviations from the equilibrium, deviations of the order of 10% for the electric currents considered in Figure 4.

It is customary to consider the actual values of the electric currents in Figure 4 (i.e., not in units of FDc_0/δ). These currents range from 1 to 10 A/cm^2, which are much larger than those used in practical situations with synthetic membrane processes. Nevertheless, we have considered very thin, highly permeable membranes, so that these values are not really out of line. The important parameter is not the current itself but the degree of polarization of the interface. We have computed the potential

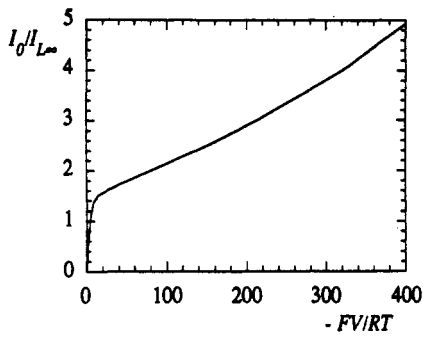

Figure 5. Steady-state current–voltage curve for a moderately charged and relatively thick membrane: $d = \delta = 10^3\lambda$, $c_0 = 0.1X$. Here V denotes $\phi(d+\delta,\infty) - \phi(-\delta,\infty)$.

differences at the interfaces of thick membranes and have also obtained 10% deviations from equilibrium when the same degree of polarization of the interface is considered, although in these cases the currents were of the order of some mA/cm². It is worth indicating that this definition of the "nonequilibrium Donnan potential" is not convenient when high degrees of polarization are involved. For instance, when the electric current is half the limiting current, deviations from the equilibrium Donnan potential can be as large as 50% (left) and 20% (right), but the computed potential differences may contain a 10% error. This can be understood if we recall that the electric potential profile is far from linear near the left interface, where the ionic concentrations are greatly diminished.

Note that we could also define a "nonequilibrium Donnan potential" as the jump in electric potential that arises from the extrapolation of the ion concentration profiles using the Boltzmann law. This would lead to two new definitions, depending on the use of either the counterion or the co-ion profile. The results obtained using these definitions quantitatively validate the deviations mentioned above (Figure 2 can be used to check this assertion), and they also show new interesting phenomena. The deviations from the equilibrium Donnan potential seem to be higher for the counterion than for the co-ion, a behavior that can be easily explained by the fact that the deviations from the equilibrium Donnan potential are due to the fluxes, and the counterion flux is greater than the co-ion flux. However, our present calculations do not allow quantitative estimation of this effect. More refined calculations, aimed specifically at showing this effect are required.

Figure 5 shows the steady-state current–voltage characteristic for a relatively thick membrane having $d = \delta = 10^3\lambda$, and a fixed charge concentration 10 times that of the bulk electrolyte, $X = 10c_0$. This curve can be compared with those appearing in ref 3, but it should be noted that Figure 5 refers to the *whole* membrane system, while those in ref 3 refer only to the left DBL. It can also be compared with experimental characteristics[4] if correction is made for the ohmic drop in the bulk solutions normally included in the experimental curves. The limiting current can be *estimated* theoretically as the current that leads to zero concentration at the left membrane/solution interface when the electroneutrality condition is employed to describe transport in the DBL. Thus, eq 10 yields

$$0 = c_0 - \frac{J_1 + J_2}{2D}\delta \tag{11}$$

which can be combined with the equation for the steady-state electric current

$$I = F(J_1 - J_2) \tag{12}$$

to obtain the result

$$I_L = \frac{J_1 - J_2}{J_1 + J_2}\frac{2FDc_0}{\delta} = \frac{\eta_s + 1}{\eta_s - 1}\frac{2FDc_0}{\delta} \tag{13}$$

where $\eta_s = -J_1/J_2$ is a parameter closely related to the permselectivity of the membrane system. Note that the classical theory of concentration polarization makes use of the assumption of *ideal* permselectivity of the membrane system ($\eta_s \to \infty$) in order to write

$$I_{L\infty} = 2FDc_0/\delta \tag{14}$$

for the limiting current. Other treatments assume that the permselectivity of the membrane system is known and use $I_{L\infty}$ in eq 13 as the theoretical value for the limiting current. However, it should be noticed that the permselectivity of the *membrane system* is *not* the permselectivity of the *membrane* and that the actual permselectivity of the membrane or the membrane system cannot be predicted theoretically in the presence of an electric current.[15] This can be explained as follows. If we eliminate the electric potential gradients from the Nernst–Planck equations we obtain

$$J_1c_2 + J_2c_1 + D\frac{\partial(c_1c_2)}{\partial x} = 0 \tag{15}$$

Integration of eq 15 from $x = -\delta$ to $x = d + \delta$ yields the interesting result

$$\eta_s = \langle c_1\rangle_s/\langle c_2\rangle_s \tag{16}$$

where $\langle\ \rangle_s$ denotes the concentration averaged over the entire membrane system. (The validity of this equation was checked in all of our computations.) The boundary conditions imposed on the transport problem allow for ion fluxes through the outer boundaries of the system. Therefore, during the transient regime, when the fluxes entering the system can differ from those leaving it, the average ion concentrations can vary. The result is that η (i.e., the permselectivity of the membrane system) may depend on the magnitude of the current. However, in the underlimiting current regime, the actual changes in these average magnitudes are very small. In this case, eqs 10 can be used to estimate the average ion concentrations in the DBLs and, then, eq 16 can be transformed into

$$\eta_s = \frac{\langle c_1\rangle_m + \dfrac{2c_0\delta}{d}}{\langle c_2\rangle_m + \dfrac{2c_0\delta}{d}} \neq \frac{\langle c_1\rangle_m}{\langle c_2\rangle_m} \equiv \eta_m \tag{17}$$

where $\langle\ \rangle_m$ denotes the concentration averaged only over the membrane. Equation 17 indicates that the permselectivity of the membrane system is that of the membrane ($\eta_s \approx \eta_m$) when transport is totally controlled by the membrane, and that of the solution ($\eta_s \approx 1$, i.e., no permselectivity) when the transport is totally controlled by the DBLs.[7] However, in most practical cases the situation is not so simple. The counterion concentration in the membrane system is usually determined by the membrane, but the co-ion concentration is determined by the DBLs. In other words, transport in the DBL is the rate-determining step for counterions while transport in the membrane is rate-determining for the co-ions. It is this important effect of the DBLs on the determination of $\langle c_2\rangle_s$ that makes it inaccurate to approximate the permselectivity of the membrane system as that of the membrane. Thus, for the conditions given in Figure 6 and $I_0 = 0$, $\eta_s = 5.8$ while $\eta_m = 101$. At $I_0 \approx 1.5I_{L\infty}$, $\eta_s = 5.5$ and $\eta_m = 4$. For the case under discussion we can estimate the actual limiting current of the membrane system by making use of eq 13 and the value $\eta_s = 5.5$ as $I_L \approx 1.45I_{L\infty}$ (see Figure 5).

Finally, Figure 6 shows the profile of the steady-state space-charge concentration in the left DBL (a) and the two membrane/solution interfaces (b), for different values of $I_0/I_{L\infty}$: 0, 0.5, 1.5, 2.5, and 5. This figure confirms results obtained previously by Rubinstein[3] and Gurevich et al.[16] in membrane systems, and by Buck[10] in electrode systems, on the occurrence of a maximum in the space-charge distribution. However, since we have considered the nonequilibrium diffuse double layers in the *whole* membrane

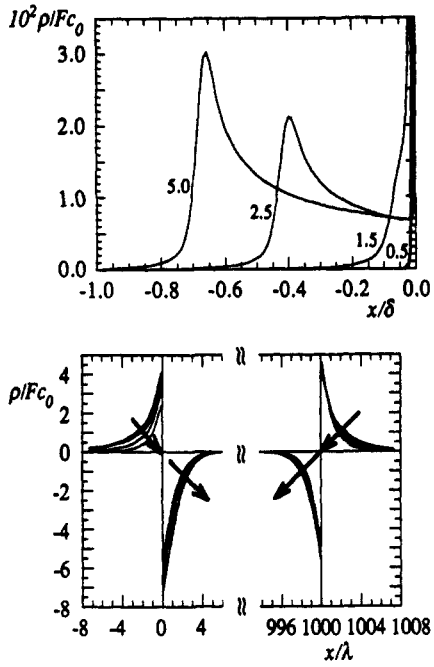

Figure 6. (a, top) Steady-state space-charge concentration profiles for the conditions of Figure 5 and the following values of the electric current: $I_0/I_{L\infty}$ = 0, 0.5, 1.5, 2.5, and 5. (b, bottom) Detail of the space-charge concentration profiles at the two membrane/solution interfacial regions corresponding to the profiles in Figure 6a. The arrows indicate increasing values of $I_0/I_{L\infty}$.

system, a more detailed explanation of the phenomena can now be given. (This kind of study is not usual in the literature: diffuse double layer studies generally assume that the system is in equilibrium,[14] transport studies assume that local equilibrium is established across the interface and therefore, by necessity, throughout the interfacial regions.[1,17] Furthermore, when both diffuse double layer and transport effects are considered, only part of the membrane system is studied.[3,9,18]

When $I_0 = 0.5I_{L\infty}$, the nonequilibrium double layers at the two interfaces are very similar to those at equilibrium. However, when $I_0 = 1.5I_{L\infty} \approx I_L$ the diffuse layer in the solution phase of the left membrane/solution interfacial region begins to split into two parts (see the corresponding curve in Figure 6a). As the current is increased beyond the limiting value, part of the charge in this diffuse layer remains very close to the interface but the rest spreads over the DBL (see the curves for $I_0/I_{L\infty}$ = 2.5 and 5 in Figure 6a). We will refer to the latter as the macroscopic space-charge region (SCR). Region $-8\lambda \le x \le 0$ in Figure 6b shows that the charge that remains near the interface decreases when the electric current is increased because this charge is needed in the SCR during its expansion over the DBL. The idea of splitting the diffuse double layer in two parts was first suggested by Nikonenko et al.[18] However, these authors assumed that the part of this layer remaining close to the interface could be considered as an *equilibrium* diffuse double layer. Figure 6b shows that this layer also changes with current. In defense of these authors, it must be borne in mind that ref 18 was one of the first attempts to provide an analytical solution to the problem and, at the time, some unfounded assumptions had to be used.

It is important to note that the existence of the macroscopic SCR makes feasible the passage of currents higher than the limiting current in two ways. On the one hand, it reduces the effective thickness of the electrically neutral DBL and leads to an enhancement of the ion fluxes in this region.[18] On the other hand, it creates a high electric field in the SCR itself that forces the ion concentrations there to differ from zero and the ion fluxes to be the same as the rest of the membrane system. In other words, the passage of currents higher than the limiting current necessarily implies the existence of a region where the ion concentrations are much smaller than in the rest of the system. The only way to have the same ion fluxes while reducing the concentrations is to increase the electric field, which in turn can be done by a volume space charge. Then, it results that the ion concentrations are decreased in this region but not at the same rate so that this region becomes a SCR. Indeed, if we do not make use of the local electroneutrality assumption in order to derive the ion concentration profiles in the DBLs (see eq 10) we obtain[3,4,9]

$$\frac{1}{2}(c_1 + c_2) = c_0 - \frac{J_1 + J_2}{2D}(x + \delta) + \frac{\epsilon}{4RT}[E^2(x) - E^2(-\delta)], \quad -\delta \le x < 0 \quad (18)$$

where $E \equiv -\partial\phi/\partial x$ is the electric field. The classical theory of concentration polarization neglects the effect of the electric field and leads to a zero value for the ion concentration at the limiting current. However, the appearance of space charge makes the electric field so large that the left hand side of eq 18 assumes a value much smaller than c_0 in the SCR but never vanishes, in agreement with experimental observations.[19] For instance, for the conditions given in Figure 5 and with $I_0 = 5I_{L\infty}$, we find $(J_1 + J_2) = 2.97I_{L\infty}/F$ and $E(-\delta) = 5(RT/F\delta)$ (negligible). And at $x = -\delta/2$, $c_1 + c_2 = 2.2 \times 10^{-2}c_0$ and $E = 0.445 \times 10^3(RT/F\delta)$. In conclusion, we can clearly identify two regions in the DBL. In the left portion of this layer transport is basically electroneutral and can be described by eq 18, while the right portion evolves into a macroscopic SCR where the electric field is so high that the transport is due to ion migration.[5] The relative extensions of these two regions vary with the electric current as is shown in Figure 6a.

Region $0 \le x \le 8\lambda$ in Figure 6b shows that the splitting of the diffuse layer in the solution phase is also accompanied by greater charge separation at the interface. That is, the macroscopic SCR takes charge from the diffuse layer and this layer, in turn, takes charge from the membrane phase, thus increasing the charge separation at this interface. Finally, region $992\lambda \le x \le 1008\lambda$ in Figure 6b shows that the charge separation at the right boundary decreases when the current is increased.

Discussion

We have studied the physical state of the nonequilibrium diffuse double layer at the ion-exchange membrane/solution interface during the passage of electric current. The *entire* membrane *system* rather than only the polarized DBL has been studied. Interesting results arise due to the nonlinear character of the system of equations consisting of the Nernst–Planck and Poisson equations, and the inhomogeneous nature of the membrane system (membrane plus bathing solutions). Some of these results confirm previous results obtained using different methods.[3,10] Others provide new physical insights into problems such as the question of the validity of the equilibrium Donnan relations, and the permselectivity of charged membranes.

The problem we have addressed here is so difficult in its own right that consideration of additional effects would certainly obscure the conclusions obtained. We have carried out a simplified study and then some limitations should be kept in mind. *Compact* double layer effects are not accounted for. This is very usual in the membrane literature, but a careful study establishing its role in transport processes is still lacking. Also, we stated in the Introduction that only cation-exchange membranes would be dealt with because we wished to ignore water dissociation effects. Water dissociation in bipolar ion-exchange membranes[20] seems to demand fields of at least 10^8–10^9 V/m and appears predominantly in the anion-exchange layers. The fields which typically appear in this study are of the order of 10^7–10^8 V/m. However, greater fields could be found for high enough electric currents. The question is whether they are *realistic*: very high values of E must

certainly promote convective movements of the fluid that will act to decrease the huge electrical energy stored in the system (see refs 21 and 22). Yet, these movements are not *allowed* in our model.

Let us consider now these convective effects in more detail. We have estimated the Joule heating of the SCR, for $I_0 = 5I_{L\infty}$ together with the conditions of Figure 5, to approximate 10 W/cm^2, which would lead to a temperature gradient of some 0.2 °C/μm in that region, if the heat were to be dissipated only by conduction. This gradient is important and could give rise to thermal convection. Some comments must be added concerning the magnitude of this temperature gradient. Even though these numbers and Figure 5 refer to a relatively thick membrane, the thickness is still unrealistic. This leads to a limiting current at least 1 order of magnitude larger than in the case of real synthetic membranes and, then, to a difference of at least 2 orders of magnitude in the estimation of the Joule heating. Previous estimates of the importance of the thermal convection due to Joule heating have found this effect unimportant.[21,23] In any event, it seems quite possible that the considerable charge separation obtained in the polarized DBL, at high currents, should trigger other processes[4,11,22] that will couple with those of electrodiffusion treated here. By proceeding in this way, the system could minimize the huge electrical energy accumulated throughout macroscopic regions. It was first suggested in ref 23, and carefully studied in refs 24, that conductive inhomogeneities at the membrane surface may provide a basis for an electroconvective process. Still, the present study is one of the few that have been performed in which nonequilibrium space-charge effects are considered within the context of the *whole membrane system*. Indeed, the classical literature of transport phenomena through charged membranes[7,17] has not dealt with the detailed role of the interfaces because the main resistance to transport was assumed to be due to the membrane bulk. In 1968 MacGillivray already showed[25] that this was a safe assumption as long as the membrane thickness was much greater than those of the interfacial regions (typically several Debye lengths). Only recently[1,3,11,26] has it been appreciated that a complete understanding of transport phenomena in charged membranes must consider the interfacial regions in more detail than previously.

Finally, as an addendum, we should note that the assumption of local (Donnan) equilibrium at an interface, during charge transport, is equivalent to the assumption of constant quasi-Fermi level for the majority carrier in a semiconductor[27] where the relevant differential equations are often identical with those treated in this paper. Thus, our nonequilibrium methods and results should be of interest to semiconductor device technology.

Acknowledgment. We thank again Dr. Alan Hindmarsh of the Lawrence Livermore National Laboratory for providing us with his ODE integrator LSODI as well as many others from ODEPACK in the early 1980s. Financial support from the National Science Foundation (CHE90-22215), the Dirección General de Investigación Científica y Técnica (PB92-0516-C), the University of Valencia (S.M.), and the Spanish–Northamerican Committee for Cultural, Educational and Scientific Cooperation (J.A.M.) is gratefully acknowledged.

Appendix

The numerical procedure employed is the method of lines that was thoroughly discussed in ref 2. Since this procedure permits the introduction of initial discontinuities in the variables, it can be (and is) used to solve the two problems discussed above. We provide a brief outline of the method below.

Let the interval $[-\delta, d+\delta]$ be divided into a sequence of points, NPT in number, such that

$$-\delta = x_1 < x_2 < \ldots < x_{NPT} = d + \delta \qquad \text{(A1)}$$

Using centered differences, the spatial derivatives in eqs 4 and 5 are discretized (see ref 2 for the actual difference formulas). The Dirichlet condition $\phi(-\delta,t) = 0$ is incorporated into the algorithm by adding the dummy equation $d\phi_1/dt = 0$, where $\phi_1 \equiv \phi(x_1,t)$. The spatial discretization of eq 7 uses one-sided differences, e.g.,

$$\left(\frac{\partial c_2}{\partial x}\right)_{NPT} = \frac{c_{2\,NPT} - c_{2\,NPT-1}}{x_{NPT} - x_{NPT-1}} \qquad \text{(A2)}$$

etc.

Define the solution vector y as

$$\mathbf{y}^T = (c_{11}, c_{21}, \phi_1, c_{12}, c_{22}, \phi_2, \ldots, c_{1NPT}, c_{2NPT}, \phi_{NPT}) \qquad \text{(A3)}$$

for the first problem (formation of the equilibrium EDL) and

$$\mathbf{y}^T = (c_{11}, c_{21}, \phi_1, c_{12}, c_{22}, \phi_2, \ldots, c_{1NPT}, c_{2NPT}, \phi_{NPT}, (\partial\phi/\partial x)_{NPT}) \qquad \text{(A4)}$$

for the nonequilibrium EDL problem. Here T denotes the transpose operator and $(\partial\phi/\partial x)_{NPT} \equiv (\partial\phi/\partial x)(d+\delta,t)$. Using the above discretization techniques in the spatial variable x (applying the method of lines) we obtain the differential-algebraic system

$$\mathbf{A}\frac{d\mathbf{y}}{dt} = f(y,t) \qquad \text{(A5)}$$

where A is the *singular* diagonal matrix

$$\mathbf{A} = \text{diag}(1, 1, 1, 1, 1, 0, 1, 1, 0, \ldots, 1, 1, 0) \qquad \text{(A6)}$$

for the generation of the initial profiles (equilibrium EDL problem), and

$$\mathbf{A} = \text{diag}(1, 1, 1, 1, 1, 0, 1, 1, 0, \ldots, 1, 1, 0, 1) \qquad \text{(A7)}$$

for the perturbation of the equilibrium profile due to the electric current (nonequilibrium EDL problem). The zeros in eqs A6 and A7 occur because the Poisson equation (4) has no time derivative and, consequently, yields an algebraic rather than a differential system in eq A5. The third 1 in eq A6 comes from the dummy equation $d\phi_1/dt = 0$ and the first three 1s in eq A7 come from $dc_{11}/dt = 0$, $dc_{21}/dt = 0$, and $d\phi_1/dt = 0$, respectively. The last 1 in eq A7 comes from the discretization of eq 7.

The system of eqs A5–A7 is stiff, but standard stiff integrators are not applicable because A is singular. Instead, we make use of the software package LSODI, which contains Gear's stiffly stable difference operators of order 1–5 and can solve the above system even when A is singular. LSODI is a variable order and variable step size integrator that monitors the error growth by comparing the differences between predictor and corrector equations with the truncation errors for various orders. This integrator uses the *numerically* generated Jacobian $(\partial f/\partial y)$ to form a pseudo-Newton's method to converge the corrector equation. Newton-like iterative methods rather than simple ones are required because of the stiffness of the system. The algorithm makes use of the fact that this Jacobian matrix is banded with a half-bandwith equal to 5. In general, when other ionic systems are studied, the bandwidth is equal to 2NDPE – 1, where NPDE is the number of PDEs. The actual pseudo-Newton's method uses the *non-singular* matrix $\mathbf{A} - \Delta\tau\beta_k(\partial f/\partial y)$, where Δt is the step size and β_k $(1 \le k \le 5)$ is a constant related to the kth order of the corrector equation.

The values for $(dy/dt)(0)$ (required by LSODI) are obtained from $f(y(0),0)$ for all non-ϕ components, and the following equations

$$\frac{\partial\phi}{\partial t}(x,0) = 0 \qquad \text{(A8)}$$

$$\frac{\partial}{\partial t}\left(\frac{\partial\phi}{\partial x}\right)(d+\delta,0) = 0 \qquad \text{(A9)}$$

The main advantage of this approach over a more classical procedure is that the step size Δt and the order of the numerical method (first to fifth) are automatically adjusted to guarantee that a relative and/or absolute error tolerance is satisfied. This is especially important in regions of large gradients or when large values of Δt are required to reach the steady state.

The integral boundary condition shown in Figure 1 is handled in a natural way with this software package as the differential equation, eq 3. The latter is integrated using the same order of difference scheme as the other equations in eq A5. This approach yields a much more stable algorithm than the one that would result if the integral boundary condition were integrated using the trapezoidal rule of some other fixed quadrature formula.

The code imposes no requirements on the spatial grid. However, any particular choice should consider the presence of the two membrane/solution interfaces (where large gradients in the physical variables are expected) and should be useful for the study of both thick and thin membranes, in the sublimiting and overlimiting current regimes. Also, a continuous variation of the step size with small steps at the two outer boundaries (where the boundary conditions are imposed) is preferred. Our choice is symmetrical about $x = d/2$ and includes two parameters: the number of grid points in each one of the bathing solutions (NL) and in the membrane (NW). The grid is defined in the region $-\delta \le x \le d/2$ as

$$x_i = \begin{cases} -\delta + (i-1)\left[\dfrac{8\lambda}{\frac{NW}{2}} + \dfrac{(i-2)\lambda}{\frac{NL}{2} - \frac{NW}{8} - 1}\left(\dfrac{\frac{\delta}{2} - 2\lambda}{\frac{NL}{2} - \frac{NW}{8}} - \dfrac{8\lambda}{\frac{NW}{2}}\right)\right], & 1 \le i \le \dfrac{NL}{2} - \dfrac{NW}{8} + 1 \\ -\delta - 4\lambda - x_j, \quad \text{where } j = NL - \dfrac{NW}{4} + 2 - i, & \dfrac{NL}{2} - \dfrac{NW}{8} + 2 \le i \le NL - \dfrac{NW}{4} \\ -4\lambda + \left(i - NL + \dfrac{NW}{4} - 1\right)\dfrac{8\lambda}{\frac{NW}{2}}, & NL - \dfrac{NW}{4} + 1 \le i \le NL + \dfrac{NW}{4} + 1 \\ -4\lambda + \left(i - NL + \dfrac{NW}{4} - 1\right)\left[\dfrac{8\lambda}{\frac{NW}{2}} + \dfrac{i - NL + \frac{NW}{4} - 2}{\frac{NW}{4} - 1}\left(\dfrac{\frac{d}{2} - 4\lambda}{\frac{NW}{4}} - \dfrac{8\lambda}{\frac{NW}{2}}\right)\right], & NL + \dfrac{NW}{4} + 2 \le i \le \dfrac{NPT + 1}{2} \end{cases} \tag{A10}$$

This grid has a step size $\Delta x = (16/NW)\,\lambda$ at the two outer boundaries $x = -\delta$ and $x = d + \delta$. Here λ is the Debye length in the membrane solution. This is also the case for the membrane/solution interfacial regions. The grid takes into account that these regions have a size of about 8λ (four Debye lengths in each phase). Note that this is *not* a physical requirement imposed on the system, but a procedure to incorporate in the grid the fact that the electric double layer usually extends over a few Debye lengths. The grid is stretched linearly in the other regions, thus satisfying the condition of "continuity" for the step size. The values NL = 250 and NW = 200 have proved to be suitable for all the situations that we considered. The total number of points is then NPT = 2NL + NW + 1. Note, finally, that this particular grid cannot be used for $d \le 12\lambda$ (a case far from our interest) nor with values of NL such that the ratio NW/NL > 4.

References and Notes

(1) Bassignana, I. C.; Reiss, H. *J. Phys. Chem.* **1983**, *87*, 136. Selvey, C.; Reiss, H. *J. Membr. Sci.* **1987**, *30*, 75.

(2) Murphy, W. D.; Manzanares, J. A.; Mafé, S.; Reiss, H. *J. Phys. Chem.* **1992**, *96*, 9983.

(3) Rubinstein, I. *Electro-Diffusion of Ions*; SIAM Studies in Applied Mathematics: Philadelphia, 1990.

(4) Manzanares, J. A.; Kontturi, K.; Mafé, S.; Aguilella, V. M.; Pellicer, J. *Acta Chem. Scand.* **1991**, *45*, 115.

(5) Listovnichii, A. V. Élektrokhimiya **1991**, *27*, 316 [*Sov. Electrochem.* **1991**, *27*, 284].

(6) Hainsworth, A. H.; Hladky, S. B. *Biophys. J.* **1987**, *51*, 27.

(7) Helfferich, F. *Ion Exchange*; McGraw-Hill: New York, 1962.

(8) Jonsson, G.; Boessen, C. In *Synthetic Membrane Processes*; Belfort, G., Ed.; Academic Press: New York, 1984; pp 101–30.

(9) Spaarnay, M. J. *Trans. Faraday Soc.* **1957**, *53*, 306. Bass, L. *Ibid.* **1964**, *60*, 1656. Newman, J. *Ibid.* **1965**, *61*, 2229. Symrl, W. H.; Newman, J. *Ibid.* **1966**, *62*, 207.

(10) Buck, R. P. *J. Electroanal. Chem.* **1973**, *46*, 1.

(11) Fang, Y.; Li, Q., Green, M. E. *J. Colloid Interface Sci.* **1982**, *86*, 185. Fang, Y.; Li, Q., Green, M. E. *J. Colloid Interface Sci.* **1982**, *88*, 214. Green, M. E.; Rodney, R. *J. Phys. Chem.* **1987**, *91*, 1797.

(12) Brumleve, T. R.; Buck, R. P. *J. Electroanal. Chem.* **1978**, *90*, 1.

(13) The incorporation of the equilibrium EDL in the initial state of the problem is not mere refinement. In fact, this is the proper way of establishing a consistent physics for membrane problems. Furthermore, this approach has also proved to be necessary in the study reported in ref 1.

(14) Manzanares, J. A.; Mafé, S.; Bisquert, J. *Ber. Bunsenges. Phys. Chem.* **1992**, *96*, 538.

(15) Manzanares, J. A.; Mafé, S.; Pellicer, J. *J. Chem. Soc., Faraday Trans.* **1992**, *88*, 2355.

(16) Gurevich, Yu. Ya.; Noskov, A. V.; Kharkats, Yu. I. Élektrokhimiya **1991**, *27*, 667 [*Sov. Electrochem.* **1991**, *27*, 605].

(17) Lakshminarayanaiah, N. *Transport Phenomena in Membranes*; Academic Press: New York, 1969.

(18) Nikonenko, V. V.; Zabolotskii, V. I.; Gnusin, N. P. Élektrokhimiya **1989**, *25*, 301 [*Sov. Electrochem.* **1989**, *25*, 262].

(19) Forgacs, C.; Leibovitz, J.; O'Brien, R. N.; Spiegler, K. S. *Electrochim. Acta* **1975**, *20*, 555. Khedr, G.; Varoqui, R. *Ber. Bunsenges. Phys. Chem.* **1981**, *85*, 116.

(20) Ramírez, P.; Rapp, H. J.; Reichle, S.; Strathmann, H.; Mafé, S. *J. Appl. Phys.* **1992**, *72*, 259.

(21) Lifson, S.; Gavish, B.; Reich, S. *Biophys. Struct. Mech.* **1978**, *4*, 53.

(22) Reich, S. *Appl. Phys. Lett.* **1978**, *33*, 988.

(23) Rubinstein, I.; Staude, E.; Kedem, O. *Desalination* **1988**, *69*, 101.

(24) Rubinstein, I.; Maletzki, F. *J. Chem. Soc., Faraday Trans.* **1991**, *87*, 2079. Maletzki, F.; Rösler, H.-W.; Staude, E. *J. Membr. Sci.* **1992**, *71*, 105.

(25) MacGillivray, A. D. *J. Chem. Phys.* **1968**, *48*, 2903.

(26) Timashev, S. F. *Physical Chemistry of Membrane Processes*; Ellis Horwood: London, 1990.

(27) Grove, A. S. *Physics and Technology of Semiconductor Devices*; John Wiley: New York, 1967; pp 183–6. Sze, S. M. *Physics of Semiconductor Devices*; John Wiley: New York, 1981; pp 84–9. Roulson, D. J. *Bipolar Semiconductor Devices*; McGraw-Hill: New York, 1990; pp 40–8.